

ACCEPTED MANUSCRIPT

# Influence of magnetosphere disturbances on particle fluxes measured by ground-based detectors

To cite this article before publication: Ashot Chilingarian *et al* 2024 *EPL* in press <https://doi.org/10.1209/0295-5075/ad7e4c>

## Manuscript version: Accepted Manuscript

Accepted Manuscript is “the version of the article accepted for publication including all changes made as a result of the peer review process, and which may also include the addition to the article by IOP Publishing of a header, an article ID, a cover sheet and/or an ‘Accepted Manuscript’ watermark, but excluding any other editing, typesetting or other changes made by IOP Publishing and/or its licensors”

This Accepted Manuscript is **Copyright © EPLA, 2024**.



During the embargo period (the 12 month period from the publication of the Version of Record of this article), the Accepted Manuscript is fully protected by copyright and cannot be reused or reposted elsewhere.

As the Version of Record of this article is going to be / has been published on a subscription basis, this Accepted Manuscript will be available for reuse under a CC BY-NC-ND 3.0 licence after the 12 month embargo period.

After the embargo period, everyone is permitted to use copy and redistribute this article for non-commercial purposes only, provided that they adhere to all the terms of the licence <https://creativecommons.org/licenses/by-nc-nd/3.0>

Although reasonable endeavours have been taken to obtain all necessary permissions from third parties to include their copyrighted content within this article, their full citation and copyright line may not be present in this Accepted Manuscript version. Before using any content from this article, please refer to the Version of Record on IOPscience once published for full citation and copyright details, as permissions may be required. All third party content is fully copyright protected, unless specifically stated otherwise in the figure caption in the Version of Record.

View the [article online](#) for updates and enhancements.

## **Influence of Magnetosphere Disturbances on particle fluxes measured by ground-based detectors.**

*A.Chilingarian, T.Karapetyan, B.Sargsyan, K.Asatryan, G.Gabaryan*

*Yerevan Physics Institute*

*Alikhanyan Brothers 2, Yerevan, Armenia AM0036*

### **Abstract**

This study examines how the Earth's surface particle fluxes are modulated by the Interplanetary Magnetic Field (IMF) carried by Coronal Mass Ejections (ICME). Our findings underscore the role of magnetic reconnection in allowing low-energy galactic cosmic rays (GCR) to penetrate the magnetosphere, leading to enhanced secondary particle fluxes through reduced cutoff rigidity—a phenomenon known as the magnetospheric effect (ME). In contrast, the Forbush decrease (FD) driven by the scalar magnetic field strength results in significant particle flux reductions. On May 10-11, 2024, the FD, directly linked to the enormous geomagnetic storm (GMS), was complicated by the simultaneous registration of secondary particles from the Solar Energetic Particle (SEP) event, which was energetic enough to generate secondary particles in space and on the ground, leading to increases in detector count rates, known as ground-level enhancements (GLEs). Using new experimental facilities, we reveal that secondary particles during ME events release up to 10 MeV energy (maximum energy of approximately 10 MeV), whereas, during FD and GLE events, the energy release extends to 100 MeV (maximum energy of approximately 100 MeV). These insights contribute to refining event classification schemes and predictive models of space weather.

### **1. Introduction**

The solar-terrestrial relations involve variations in the intensity of neutral and charged particles measured on Earth's surface during geomagnetic storms (GMS) triggered by incoming Interplanetary Coronal Mass Ejections (ICME). The interaction between the ICME's magnetic field and Earth's geomagnetic field (GMF) disrupts the normally stable influx of GCRs, sometimes trapping low-energy particles in specific atmospheric regions or allowing their entry into otherwise restricted areas.

Cosmic rays are monitored on Earth by networks of particle detectors, which measure secondary cosmic rays produced when primary protons and stripped nuclei interact with atmospheric atoms. These networks include the largest Neutron Monitor network (NM [1]), the Solar Neutron Telescope (SNT) network [2], the SEVAN network [3], which additionally captures electron, gamma ray, and muon fluxes, Spaceship Earth [4], and the Global Muon Detector Network (GMDN [5]). The network of NMs covered almost the whole globe, from the Antarctic to the Arctic regions. SEVAN network detectors are located at mountain tops in Armenia, Germany, and Eastern Europe; other networks are located at different latitudes and longitudes. The detection of solar events is surprisingly coherent by Neutron monitors and SEVAN networks [6].

1  
2  
3  
4 The secondary particle fluxes can enhance for a few hours (magnetospheric effect, ME [7]) or  
5 deplete, with the following recovery (Forbush decrease, FD [8]). The ME is explained by the  
6 decrease of the cutoff rigidity (the minimal energy allowing galactic protons to enter the  
7 atmosphere above the detector), FD – by the emerging difficulties of entering galactic protons  
8 into the atmosphere due to magnetic traps that can deflect charged particles, impacting their  
9 entry into the atmosphere. Magnetospheric events, directly linked to GMS, can be complicated  
10 by the simultaneous registration of secondary particles from Solar Energetic Particle (SEP [9])  
11 events accelerated during intense flares. SEPs sometimes contain protons energetic enough to  
12 generate secondary particles in space [10] and on the ground, leading to increases in detector  
13 count rates, known as ground-level enhancements (GLEs [11]). GLEs typically reach detectors in  
14 a few tens of minutes after a solar flare, while the arrival time of ICME after the solar burst is  
15 much longer, from 20 hours (shortest) to 5 days [12]. The same group of solar spots can result in  
16 multiple ICMEs before the SEP event, causing overlapping FD and GLE events.  
17  
18

19  
20 Despite significant progress in understanding solar-terrestrial connections [13], there are no  
21 exhausting models of the solar wind—GMF interactions that can predict opposite effects in  
22 secondary particle flux intensity (FD or ME, [14]). Moreover, the existent ground-based particle  
23 detectors cannot measure the energy of the registered particles. The new type of measurements  
24 can help create more detailed models and better understand GCR modulation. Using a  
25 modernized SEVAN detector [15], we recently added to the CR variation research the energy  
26 release measurements of additional particles hitting the detectors during ME and GLE and the  
27 deficit of CR during FD. In this way, we access the energy of the GCR, affected by  
28 magnetosphere disturbances and energies of solar particles, that generated secondaries registered  
29 by ground-based detectors. Our analysis of the November 2023 and May 2024 events  
30 concentrated on implementing new experimental methods, underscoring the importance of  
31 advanced measurement techniques in studying solar-terrestrial relations.  
32  
33  
34  
35

## 36 2. Methods

37

38 The SEVAN (Space Environment Viewing and Analysis Network) consists of particle detectors  
39 strategically placed at middle to low latitudes, primarily on mountain peaks [3]. These detectors,  
40 operational for nearly 15 years, now include the SEVAN-light modules, which can measure  
41 particle energy release in the 5–100 MeV range, significantly improving over previous just count  
42 rate measurements.  
43

44 The SEVAN modules contain three layers of particle detectors interlayered by lead absorbers to  
45 be compatible with neutron monitors. Upper and lower scintillators are 5 cm thick and 1 m<sup>2</sup> in  
46 area, and the middle detectors are 25 cm. thick and 0.25 m<sup>2</sup> in area (see details in [16]). SEVAN  
47 electronics counts all possible coincidences of scintillator pulses, selecting enriched by neutral  
48 and charged particle subsamples. However, after recognizing that charged fluxes are as sensible  
49 to solar modulation as neutrons, we commissioned new SEVAN-light detectors with two layers  
50 without lead (see Fig. 1). Also, SEVAN's electronics board was updated with a new capability to  
51 measure and store energy-release histograms of charged and neutral particles each minute. The  
52 logarithmic amplitude-to-digital converter (ADC) provides linearity in the energy range from 5  
53 to 100 MeV (see Fig.4 of [17]). The upper scintillator's efficiency in registering charged particles  
54  
55  
56  
57  
58  
59  
60

is  $\approx 99\%$ , and neutral is less than 2%. Using the veto signal from the upper thin scintillator, the detector separates charged and neutral fluxes: "01" coincidence - the neutral particles, and "11" - charged particles. Correspondingly, the energy releases of charged and neutral particles are stored each minute.

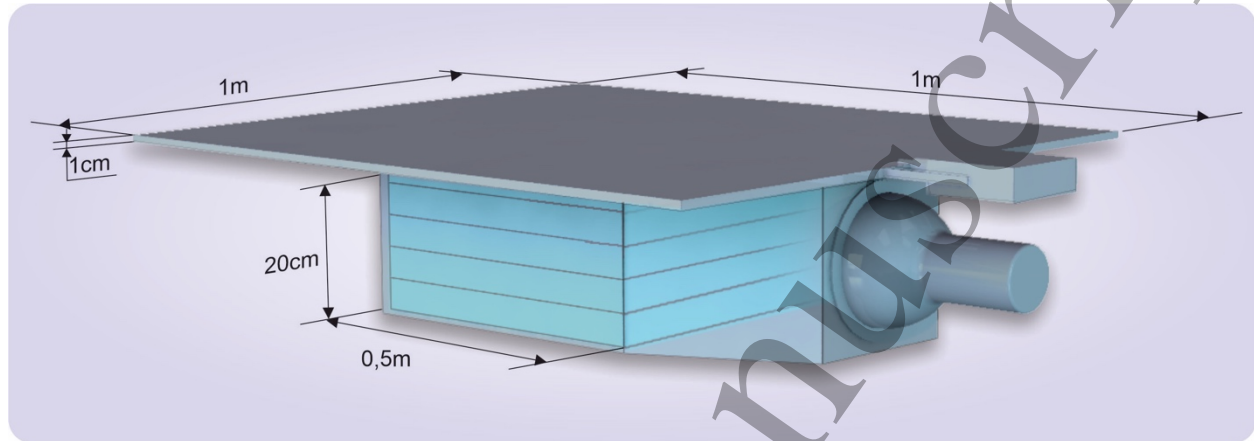


**Figure 1. Detector SEVAN-light measuring charged and neutral species of cosmic rays and their energy releases.**

The list of available information from SEVAN-light will be as follows:

- 1-minute count rates of stacked 1 and 20-cm thick scintillators.
- 1-minute count rates of the coincidences "01", signal only in 20 cm scintillator; "10" – signal only in the upper 1-cm thick scintillator, and "11" – signal in both scintillators.
- Histograms of energy releases in the thick scintillator correspond to the abovementioned coincidences.

Table 1 shows the results of the SEVAN-light detector response calculation with the simulated cosmic ray flux on Aragats. As we can see in Table 1, the "01" coincidence (signal only in the bottom scintillator) comprises  $\approx 32\%$  of neutrons and  $\approx 64\%$  of gamma rays. The contamination of charged particles is negligible; thus, with the "01" coincidence, we achieve a large purity of selected neutral particles. The "11" coincidence selects  $\approx 63\%$  of negative and positive muons and  $\approx 23\%$  of electrons and positrons; the share of neutral particles is  $\approx 8\%$ . Consequently, by the "11" coincidence, we select charged particles. Thus, using a SEVAN-light detector, we separate neutral and charged fluxes and measure the energy releases of each separately.

**Table 1. The share of cosmic ray species selected by different coincidences of the SEVAN-light detector in percent.**

SEVAN-light	Neutron (%)	Proton (%)	mu+ (%)	mu- (%)	e- (%)	e+ (%)	gamma ray (%)
Coin. "01" neutral	32,1	0,3	1,0	0,9	1,0	0,9	63,8
Coin."11" charged	1,6	6,4	33,3	29,6	12,1	10,4	6,5

The next section will demonstrate how the newly introduced energy release histograms can be applied to characterize different solar events: Forbush decreases, magnetospheric effects, and ground-level enhancements. The FDs of the 25th cycle were described in detail in [6]. In this letter, we restrict ourselves by covering particle flux disturbances of 10-11 May (FD and GLE) and their comparison with the Magnetospheric effect of November 5, 2023 [18].

### 3. Geomagnetic disturbances on May 10-11

The 25th solar activity cycle, the maximum of which is expected in 2024, brings already a series of ICMEs, SEPs, and solar particle events registered in space and on the Earth's surface. On November 5, 2023, a significant geomagnetic storm driven by a cannibal ICME interacted with Earth's magnetic field, causing a rare magnetospheric effect [18]. The G5- geomagnetic storm that occurred on May 10-11, 2024, was one of the most intense in over two decades (see detailed analysis of the event in [19]). The event unleashed deep FD, accompanied by GLE #74 in its recovery phase. Ground-based neutron monitors [20] confirmed a GLE from 02 UT on 11 May 2024, following X.5.8 flare, which reached a maximum at 01:23 UT.

In Fig.2, we show the disturbances of the X-component of the GMF measured by the Aragats magnetometer (blue), along with the SEVAN-light count rate (red) and disturbances of the near-surface electric field (black). Electric field during solar events was quiet: no thunderstorms and lightning flashes were detected. Aragats magnetometer observed storm sudden commencement (SSC) at 17:05, which triggered the extreme geomagnetic storm with a Dst index of  $-412$  nT at 2 UT on 11 May 2024, marking the sixth-largest storm since 1957 [19]. The magnetometer also shows a large compression upon the shock arrival, confirmed by THEMIS-E's and Kakioka's measurements on the magnetic field and plasma data [19].

The atmospheric electric field was calm during major geomagnetic disturbances. However, it is interesting to mention that 3 hours before SSC, at 14:00, the count rate experienced an abrupt burst, so-called thunderstorm ground enhancement (TGE, [21]) due to the strong atmospheric electric field (see the peak in the black curve at the left bottom corner).

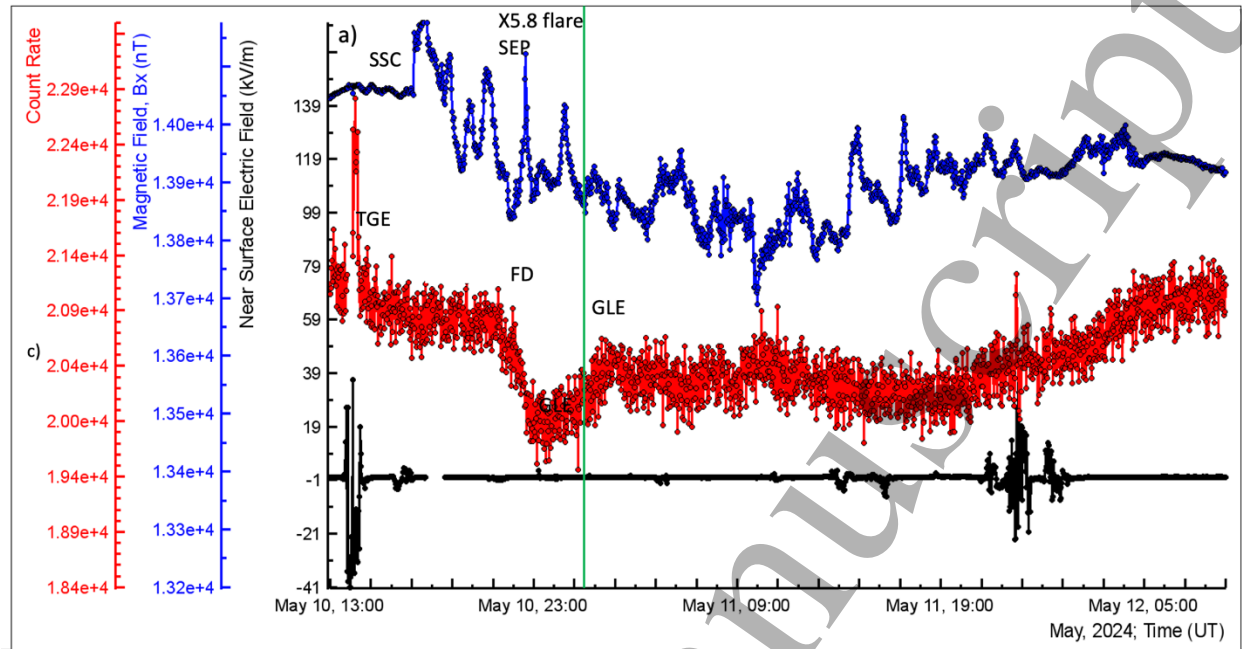


**Figure 2.** The X-component of the GMF measured by the Aragats magnetometer (blue), along with disturbances of the near-surface electric field (black) and the count rate of the SEVAN-light detector (red).

#### 4. Observation of the May events by the SEVAN network and SEVAN-light detector

In Figure 3, we present a 10-minute time series of count rates of the Nor Amberd neutron monitor (NANM) and neutral and charged fluxes selected by the coincidences of the SEVAN-light detector. Depletion of fluxes was calculated according to the mean values measured at 19:00-20:00 on May 10 (shown by the dashed lines). The FD started at  $\approx 18:30$ ,  $\approx 1.5$  hours after SSC. As was mentioned in [22], “when ICME with depleted cosmic ray flux inside passes over the Earth, ground-based monitors generally show a decrease in their flux”. Maximum depletion was  $\approx 8\%$  for the NANM and  $\approx 5\%$  for SEVAN-light, reached around midnight. Afterward, at the recovery phase, FD was interrupted by GLE after the X5.8 flare unleashed the SEP. The GLE amplitude was calculated relative to means measured at 23:00 – 24:00 on May 10.

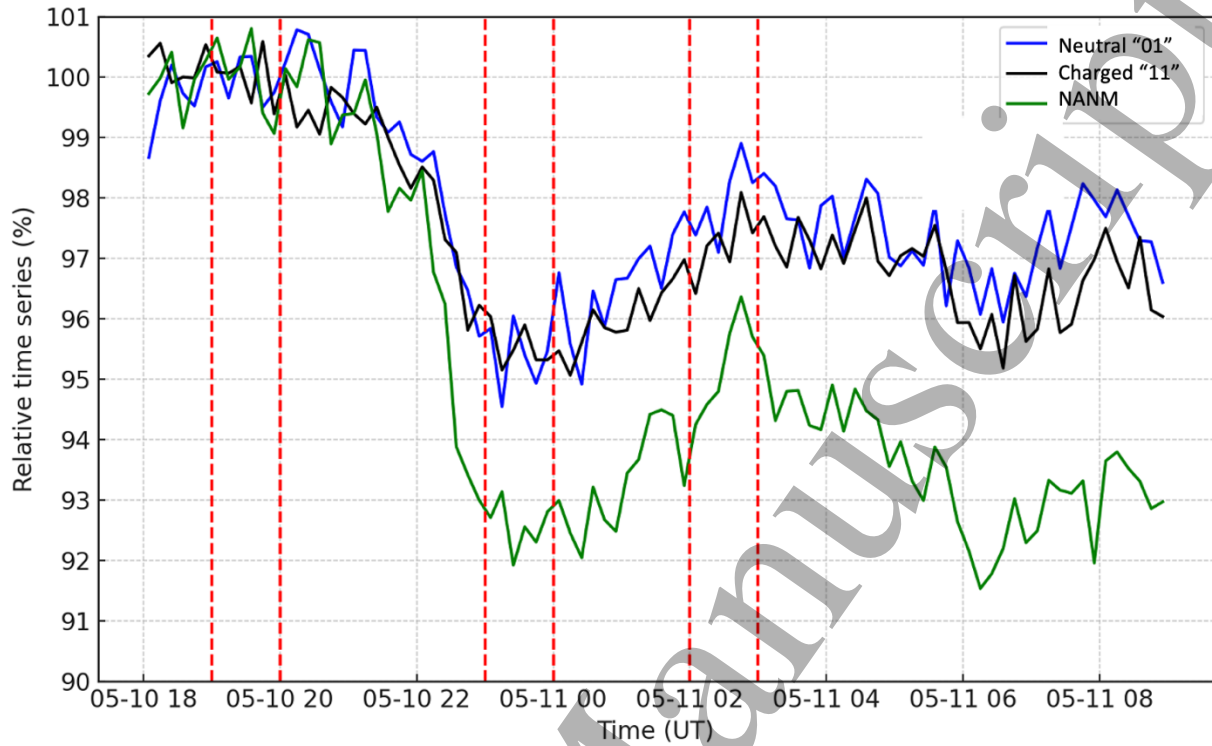


**Figure 3. Time series of count rates of Nor Amberd Neutron Monitor (NANM, green) and SEVAN-light neutral and charged particles (blue and black).**

Figure 4 demonstrates a minute time series of precise correlated counts of the 5 cm thick, 1 m<sup>2</sup> area SEVAN upper scintillators on Mts. Aragats (40.25N, 44.15E, altitude 3200 m), Musala (42.1N, 23.35E, altitude 2930 m) and Lomnický Stit (49.2N, 20.22E, altitude 2634 m).

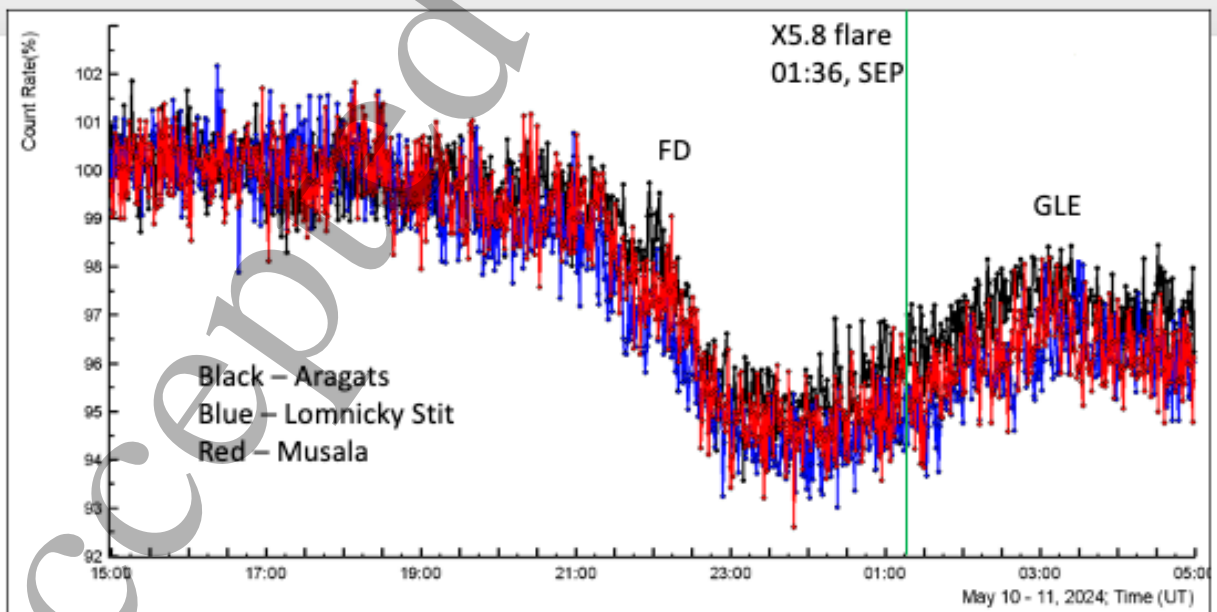


**Figure 4. Observation of FD and GLE by SEVAN network's Aragats, Lomnický Stit, and Musala detectors**

1  
2  
3  
4 Figure 5 shows the energy release histograms collected during 1 hour of maximum depletion of  
5 FD (5a, 5b) and maximum flux of GLE and ME (Figs. 5c, 5d and 5e, 5f). Histograms are  
6 obtained with the SEVAN-light detector for charged and neutral particles separately. For GLE  
7 and ME, we subtract the fair-weather histogram from the maximum flux histogram; for FD, visa  
8 verse, we subtract the maximum depletion histogram from the fair-weather histogram. The exact  
9 times are shown in Fig. 3 by dashed lines. The smooth bump in muon energy spectra is explained  
10 by electrons' and muons' most probable energy release in a 20 cm thick plastic scintillator.  
11 Assuming that the energy release in each cm of scintillator is  $\approx 2$  MeV [23],  $\approx 40$  MeV will be the  
12 most probable energy release. Charged particles can produce bremsstrahlung gamma photons,  
13 creating electron-positron pairs, thus enhancing energy release. Neutrons in the scintillator can  
14 undergo nuclear reactions, producing charged particles along their path.  
15  
16  
17  
18  
19  
20  
21  
22  
23  
24  
25  
26  
27  
28  
29  
30  
31  
32  
33  
34  
35  
36  
37  
38  
39  
40  
41  
42  
43  
44  
45  
46  
47  
48  
49  
50  
51  
52  
53  
54  
55  
56  
57  
58  
59  
60



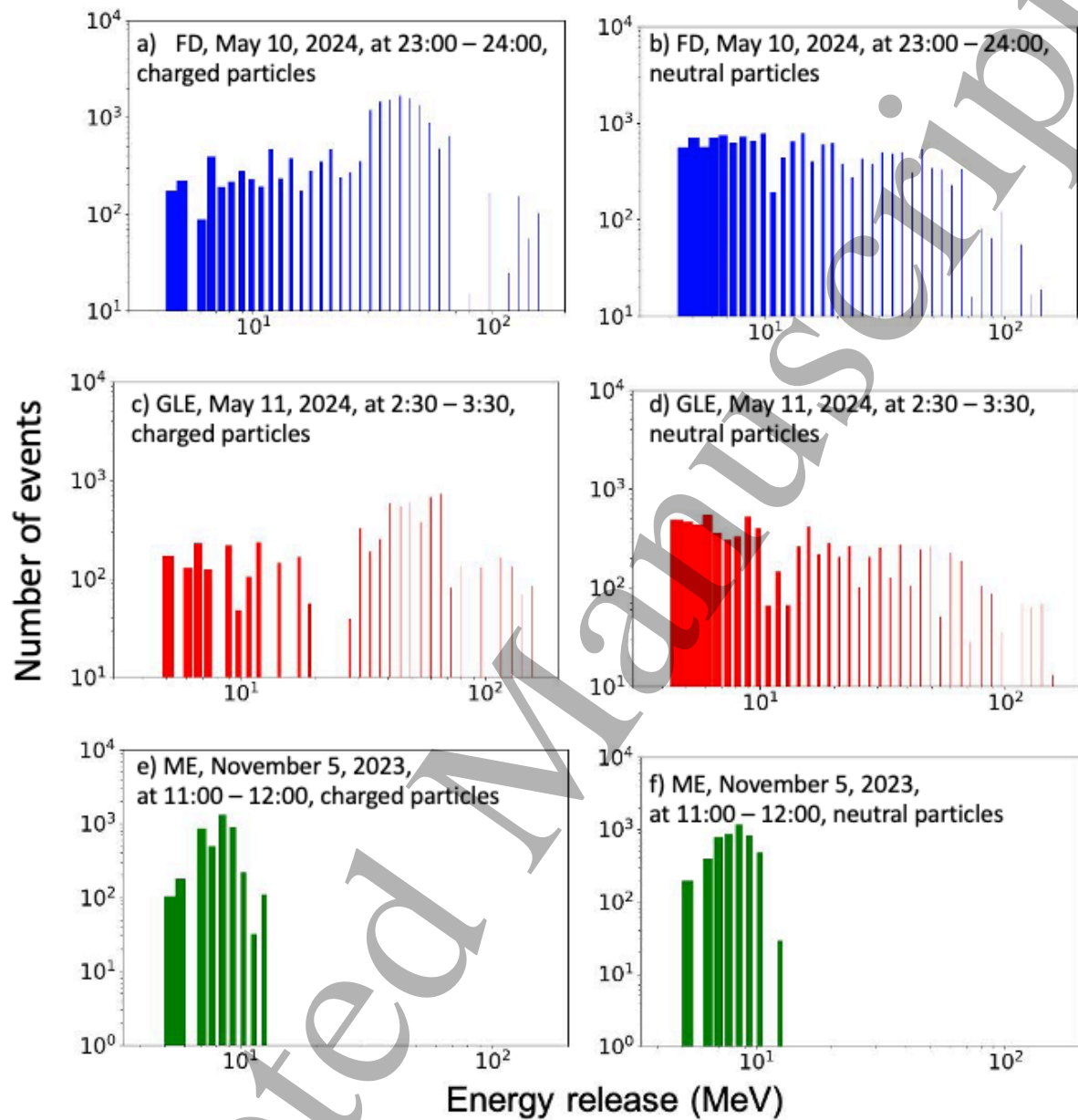


**Figure 5. The energy release histograms measured by SEVAN-light detector during three types of solar events: FD a, b), GLE c, d), and ME e, f).**

As Fig. 5 shows, the energy release histogram for the magnetospheric effect strictly differed from the ones from the FD and GLE. The energies of additional particles comprising ME (Fig 5e, 5f) are mostly lower than 10 MeV. As shown in [18], lowering the geomagnetic cutoff below 7 GeV allows low-energy GCRs to enter the atmosphere and produce showers reaching mountain altitudes. There was no flux enhancement in Arctic/Antarctic regions and on sea level. The low-energy primary protons consequently originate low-energy secondaries, which do not reach sea level and were registered by mountain-based detectors. The energy releases of secondary particles related to FD and GLE (Figs 5a, 5b and 5c, 5d) are extended to 100 MeV. Thus, galactic

and solar protons with energies higher than those that originated the ME are responsible for these events.

## 5. Discussion and Conclusions

On May 10-11, strong, coherent structures in the disturbed magnetosphere act as a barrier, reducing the influx of galactic cosmic rays causing a deep FD. Intensification of the solar wind speed and pressure compressed the magnetosphere and reduced the horizontal component of the geomagnetic field measured by ground magnetometers (upper blue curve in Fig. 2 and [19]). After dissipating these structures at the recovering phase of FD, solar protons accelerated during the X5.8 flare reach the atmosphere and initiate secondaries that reach particle detectors on the Earth's surface. The energies of GLE protons and galactic cosmic rays responsible for the Forbush decrease were above the cutoff rigidity, as we can infer by comparing energy releases of FD and GLE with ME.

When the  $B_z$  component of the ICME is southward (negative  $B_z$ ), it is opposite to the northward direction of Earth's magnetic field. This opposition facilitates magnetic reconnection on the dayside of Earth's magnetosphere, allowing solar wind energy to enter the magnetospheres. This is linked to suppressing the magnetosphere, lowering the cutoff rigidity, and allowing low-energy GCRs to enter the magnetosphere. The enhancement of the count rate of surface particle detectors at middle altitudes, and not at arctic and antarctic regions, characterized the ME. The energy releases histogram (Figs.5e, f) is a convincing confirmation of the ME, strictly differentiated from other solar-induced events.

Using the SEVAN-light detector, we measure the energy releases of neutral and charged particle fluxes. These newly established options contribute to our understanding of space weather and its potential hazards, particularly in improving the classification of solar events and refining predictive models.

## Acknowledgments

We acknowledge our colleagues from the Neutron Monitor Database (NMDB) and SEVAN Collaborations for their valuable discussions. This work was supported by the Science Committee of the Republic of Armenia, which funded Research Project No. 21AG-1C012. Data supporting this study can be accessed at <http://adei.crd.yerphi.am/>.

## References

- [1] Mishev, A., Usoskin, .I, 2020. Current status and possible extension of the global neutron monitor network, *J. Space Weather Space Clim.* 10, 17. <https://doi.org/10.1051/swsc/2020020>.
- [2] Muraki, Y., Sakakibara, S., Shibata, S., et al., 1995. New solar neutron detector and large solar flare events of June 4th and 6th, 1991. *J. Geomag. Geoelectr.* 47, 1073–1078.
- [3] Chilingarian A., G. Hovsepyan, K. Arakelyan, S. Chilingaryan, V. Danielyan, K. Avakyan, et al., Space environmental viewing and analysis network (SEVAN), *Earth Moon Planets* 104 (2009) 195.

- [4] Kuwabara, T., Bieber, J.W., Clem, J., et al., 2006. Realtime cosmic ray monitoring system for space weather. *Space Weather* 4, S08001.
- [5] Munakata, K., Bieber, J.W., Yasue, S., et al., 2000. Precursors of geomagnetic storms observed by the muon detector network. *J. Geophys. Res.* 105 (A12), 27457–27468.
- [6] Karapetyan T., Chilingarian A., Hovsepyan G., et al. The Forbush decrease observed by the SEVAN particle detector network in the 25th solar activity cycle, *Journal of Atmospheric and Solar-Terrestrial Physics* 262 (2024) 106305.
- [7] Dvornikov, V. M., V. E. Sdobnov, and A. V. Sergeev, Anomalous variations of cosmic rays in the rigidity range of 2–5 GV and their connection with heliospheric disturbances (in Russian), *Akad. Nauk SSSR Izvestiia Ser. Fizicheskaja*, 52 (1988) 2435.
- [8] Forbush S.E., World-Wide Cosmic-Ray Variations, 1937-1952, *J. Geophys. Res.*, 59 (1954) 525.
- [9] Waterfall, C. O. G., Dalla, S., Raukunen, O., Heynderickx, D., Jiggins, P., & Vainio, R., High energy solar particle events and their relationship to associated flare, CME, and GLE parameters. *Space Weather*, 21 (2023) e2022SW003334. <https://doi.org/10.1029/2022SW003334>
- [10] Koldobskiy, S., Mishev A., Fluences of solar energetic particles for last three GLE events: Comparison of different reconstruction methods, *Advances in Space Research* 70 (2022) 2585.
- [11] Poluianov, S.V., Usoskin, I.G., Mishev A.L., et al., GLE and Sub-GLE Redefinition in the Light of High-Altitude Polar Neutron Monitors, *Solar Phys* (2017) 292.  
DOI 10.1007/s11207-017-1202-4
- [12] Youssef M., Earth Moon Planets, On the Interplanetary Coronal Mass Ejection Shocks in the Vicinity of the Earth, 109, (2012) 13. DOI 10.1007/s11038-012-9398-7
- [13] Zhang, J, Temmer, M., Gopalswamy N., et al., Earth-affecting solar transients: a review of progress in solar cycle 24, *Progress in Earth and Planetary Science* 8 (2021) 56.  
[doi.org/10.1186/s40645-021-00426-7](https://doi.org/10.1186/s40645-021-00426-7)
- [14] Kudela, K., Buchik, R., Bobik P. On transmissivity of low energy cosmic rays in the disturbed magnetosphere, *Advances in Space Research* 42 (2008) 1300–1306.
- [15] Chilingarian A., Karapetyan T., Sargsyan B., Knapp J., Walter M., Rehm T., Energy spectra of the first TGE observed on Zugspitze by the SEVAN light detector compared with the energetic TGE observed on Aragats, *Astroparticle Physics* 156 (2024) 02924.
- [16] Chilingarian A., V. Babayan, T. Karapetyan, et al., The SEVAN Worldwide network of particle detectors: 10 years of operation, *Advances in Space Research* 61 (2018) 2680.
- [17] Chilingarian, A., Gharagyozyan, G., Hovsepyan, G., et al., Study of extensive air showers and primary energy spectra by MAKET-ANI detector on Mount Aragats, *Astroparticle Physics*, 28 (2007) 58.
- [18] Chilingarian A., Karapetyan T., Sargsyan B., Zazyan M., Knapp J., Walter M., Rehm T. (2024) Increase in the count rates of ground-based cosmic-ray detectors caused by the heliomagnetic disturbance on 5 November 2023 *EPL*, 146 (2024) 24001. doi: 10.1209/0295-5075/ad329c
- [19] Hayakawa *et al.*, The Solar and Geomagnetic Storms in May 2024, arXiv:2407.07665, 2024.

1  
2  
3  
4 [20] Mavromichalaki, H., Papaioannou, A., Plainaki, C., et al., Applications and usage of the  
5 real-time neutron monitor database for solar particle events monitoring. *Adv. Space Res.* 47  
6 (2011) 2210.  
7

8 [21] Chilingarian A., A. Daryan, K. Arakelyan, et al., Ground-based observations of  
9 Thunderstorm-correlated fluxes of high-energy electrons, gamma rays, and neutrons, *Phys. Rev.*  
10 *D* 82 (2010) 043009. doi: 10.1103/PhysRevD.82.043009  
11

12 [22] Raghav, A., Tari, P., Ghag, K., et al., The role of extreme geomagnetic storms in the Forbush  
13 decrease profile, *JASR* 252 (2023) 106146.  
14

15 [23] Fernow, R.C., *Introduction to Experimental Particle Physics*. Cambridge: Cambridge  
16 University Press, 1986.  
17  
18  
19  
20  
21  
22  
23  
24  
25  
26  
27  
28  
29  
30  
31  
32  
33  
34  
35  
36  
37  
38  
39  
40  
41  
42  
43  
44  
45  
46  
47  
48  
49  
50  
51  
52  
53  
54  
55  
56  
57  
58  
59  
60